Korean J. Chem. Eng., **26**(3), 833-839 (2009)

Analysis on thermal stress deformation of rotary air-preheater in a thermal power plant

Hongyue Wang*, Lingling Zhao, Zhigao Xu**, and Hyungtaek Kim*,†**

*Division of Energy System Research, Ajou University, Suwon 443-749, Korea
**College of Energy and Environment, Southeast University, Nanjing 210096, China
(*Received 10 July 2008 • accepted 3 November 2008*)

Abstract−Thermal stress deformation is a disadvantage of the rotary air preheater, which results in leakages of fluids and decrease of efficiency of the thermal system. To evaluate the results of deformation during its operation, the temperature distribution of storage materials is calculated by solving a simplified model. In this developed method, the effect of dimensionless parameters on the temperature distribution of rotary air preheater was investigated and compared with the results of modified heat transfer coefficient method. By solving coordination, structural and geometrical equations, and boundary condition in thermal-elastic theory, the thermal stress distributions in rotary air preheater are obtained in an analytical method. Experimental results are obtained by employing factorial design values of rotary air preheater for the validation of the calculation data. Good agreement has been yielded by comparing the analytical data and experimental data. Therefore, some conclusions necessary to undertake an adequate adjustment of thermal stress deformation have also been formulated, and online monitoring of the clearance of radial seals is proposed.

Key words: Rotary Air-preheater, Thermal Stress Deformation, Non-dimensional, Temperature Distribution

INTRODUCTION

1. General Characteristics of Rotary Air Preheater

Preheating of air is an effective method to obtain radiation energy efficiently by combustion. In the case of combustion with preheated air, we can get higher flame temperatures compared with ordinary combustion without preheating. Air preheating aids minimizing the heat loss from the exhaust gas, and helps to achieve a high effectiveness for the whole system. Nowadays, rotary air-preheater has been exclusively used in waste heat recovery applications for many years due to its compactness and preferable performance. As shown in Fig. 1, The heat transfer surface or elements are usually referred to as a matrix. They consist of a rotor usually made of corrugated materials which rotates at very low speeds with a constant fraction of the core facing partially for the hot fluid (gas) and cold fluid (air). The heat transfer surface area or flow passages are generally made of metals with cellular structure. When the hot gas flows over the heat transfer surface (through flow passages), the thermal energy is stored in the matrix wall. During the cold gas flow through the same passages later, the matrix wall delivers the thermal energy to the cold fluid. Thus, the specific operating principle of the rotary air-preheater is the heat transfer from the hot gas to the cold gas by means of rotating matrix. That is, heat is not transferred continuously through the wall as in a direct transfer type exchanger (recuperator), but is alternately stored and rejected by the matrix wall.

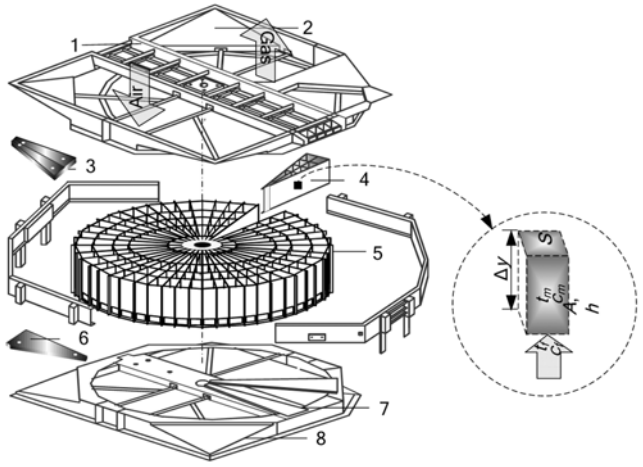

Fig. 1. The internal structure of the rotating air-preheater.

1. Upper beam	5. Rotor
2. Upper gas channels	6. Cold end sector seals
3. Hot end sector seals	7. Bottom beam
4. Segmental plate	8. Bottom gas channles

2. Technology Status of Commercialized Rotary Air Preheater

Since the rotary air-preheater operates high temperature the matrix will be expanded in the hot-gas stream and be shrinking in the cold-fluid stream. At the same time, the inlet gas temperature, gas flow rate and properties are varied momentarily; a mushroom deformation is in evitable. The result is not only the leakage but also mechanical friction which seriously affects the efficiency and security of the system. Therefore, a significant weakness of this type of heat exchanger is the unavoidable flow leakage from the clearance of the rotation matrix due to its thermal stress deformation [1-3]. It is important to pay special attention to measure mushroom deformation and adjust the sealing clearance. A lot of research was carried out by Skiepko, who studied the influence of leakage on a heat exchanger performance [4]. He presented a method for calculating the mass flows of gas through the seals [5], a method of measuring and adjusting the seal clearances in radial seals is also analyzed by him [6]. The thermal stresses and displacements that occur in an elastic hollow circular cylinder made of ceramics, when there is convective heat exchange are determined by Gromovyk [7].

†To whom correspondence should be addressed.
E-mail: htkim@ajou.ac.kr
‡This work was presented at the 7th China-Korea Workshop on Clean Energy Technology held at Taiyuan, Shanxi, China, June 26-28, 2008.

3. Outlook for Thermal Stress Deformation of Air Preheater

Engineers are interested in knowing the temperature distribution inside the air preheater in a specific period of time so they can determine the thermal stress to which the air preheater is subjected. Assuming the boundary condition are held constant during that specific period of time, the temperature inside the segmental plate of the rotary air preheater will reach certain equilibrium after some time has passed. Finding this equilibrium temperature distribution at different points on the plate is desirable, but extremely difficult. In fact, few researchers place their focus on the thermal stress deformation of air preheater; say nothing about creating methods to calculate the deformation results based on the temperature distribution. Furthermore, conventional evaluation method for the thermal deformation was not established on the temperature distribution of rotary air preheater. As segmental plate of the rotary air-preheater is welded in the center tube (see Fig. 1) and formed a rotary impeller linked with a shell, the radial thermal deformation can be treated as similar phenomena between the segmental plate and the entire rotor of air preheater [8].

In this presented study, a simplified mathematical model of segmental plate is established, thermal and stress analysis of a sheet metal in welding was investigated. Firstly, the temperature distribution within the segmental has been determined in a simplified model of the storage materials. Then, based on the theory of elasticity, the formula of the thermal stress deformation is evaluated in analytical methods. Factorial design of experiment was employed for the comparison of the calculation data. The method s suggested can be applied for determining temperature distribution and designing the thermal stress deformation of rotary air preheater which presents outline of the developed guidelines.

TEMPERATURE DISTRIBUTION IN AIR PREHEATER

1. Published on the Temperature Distribution

Analysis of temperature distribution in regenerators was initiated and developed in Germany during 1910-1930s. Prior to 1948, Hausen [10] obtained a simple approximated solution for a regenerator heat transfer model in a special condition using the finite difference technique. Creswik [10] extended this method for the unsteady state condition. Mondt [11] provided additional references on developments in the modeling with longitudinal conduction effects included in the analysis. Lambertson [12] presented a complete solution of the model for the hot and cold periods. Kays and London [13] corrected Lambertson's correlation. Bahnke and Howard [14] developed an axial conduction model for the regenerators and solved the model using the finite difference method. Razelos [16] developed an approximated method for evaluating the temperature distribution of storage metal. Djuric [16] considered thermal efficiency for the unsteady state condition. Leong and Toh [17] developed software for the regenerator simulation using the ε-NTU method. Beck [18] extended Bahnke and Howard's solution with matrix surface effects on the regenerator performance. Bahnke [19] and Howard [20] analyzed numerically the rotary regenerator problem in order to determine the regenerator heat transfer effectiveness with longitudinal conduction effect included. Skiepko [21,22] derived an analytical solution for the rotary regenerator problem including the longitudinal conduction effect in the matrix wall.

2. Simplified Model for the Temperature Distribution

In this paper, a simplified model has been established to determine the transient response of both a flat segmental plate and hollow cylindrical cross unit. Larsen [23] have presented a simplified method for the transient response of a heat storage unit initially at a uniform temperature and exposed to a step change in the inlet fluid temperature. In the simplified analysis the following assumption have been made: (1) Constant fluid and material properties; (2) Infinite thermal conductivity for the solid in the height direction; (3) Zero thermal conductivity for the solid in the radical direction; (4) Uniform heat transfer coefficient; (5) Step change in inlet fluid temperature; (6) Uniform initial temperature distribution in each storage material; (7) No heat transfer through the sides of the storage unit; (8) Constant fluid flow rate.

In fact, the transient response of the storage unit is governed by the one-dimensional conservation of energy equation for the moving fluid and the storage material. These equations can be derived by considering an incremental volume of length Δy. The energy entering the incremental volume is equal to the energy leaving plus the energy accumulated within the volume.

An energy balance for the fluid passing through the incremental volume yields

$$\frac{hA\Delta y}{L}(t_m - t_f) + m_f c_f t_f|_y = m_f c_f t_f|_{y+\Delta y} + S_f \Delta y \rho_f c_f \frac{\partial t_f}{\partial \tau} \tag{1}$$

The terms on the left-hand side of the equation represent the heat transferred from the storage material to the fluid and energy content of the fluid entering the section. These terms are equated to the energy content of the fluid leaving the section and the rate of accumulation of energy by the fluid contained within the volume. In most practical applications, compared with the other terms, the rate of accumulation of energy within the volume, the second term of the right-hand side of the Eq. (1), can be neglected. Note that

$$t_f|_y = t_f|_{y+\Delta y} + \frac{\partial t_f}{\partial y}\Delta y \tag{2}$$

The final form of the equation for the fluids is

$$\frac{m_f c_f L}{hA}\frac{\partial t_f}{\partial y} = t_m - t_f \tag{3}$$

An energy balance on the solid contained within the incremental volume can be expressed as

$$\frac{S_m \rho_m c_m L}{hA}\frac{\partial t_m}{\partial \tau} = t_f - t_m \tag{4}$$

The boundary and the initial conditions are

$$\begin{aligned} &\tau = 0 \qquad t_m = t_0 \\ &\tau > 0 \qquad t_m = (t_0 - t_{fi})\exp(\tau hA/S_m \rho_m c_m L) + t_{fi} \end{aligned} \tag{5}$$

If the following non-dimensional variables are introduced:
Non-dimensional length:

$$\xi = \frac{hAy}{m_f c_f L} \tag{6}$$

Non-dimensional time:

$$\eta=\frac{hA\tau}{S_m L\rho_m c_m} \tag{7}$$

Non-dimensional fluid temperature:

$$\theta_f=(t_f-t_0)/(t_{fi}-t_0) \tag{8}$$

Non-dimensional solid temperature:

$$\theta_m=(t_m-t_0)/(t_{fi}-t_0) \tag{9}$$

Then, the simplified mathematical model of the storage unit in non-dimensional form is

$$\begin{cases} \partial\theta_f/\partial\xi=\theta_m-\theta_f \\ \partial\theta_m/\partial\eta=\theta_f-\theta_m \end{cases} \tag{10}$$

The boundary and the initial conditions are

$$\begin{cases} \eta=0 \quad \theta_m=0 \\ \xi=0 \quad \theta_m=1.0-\exp(-\eta) \end{cases} \tag{11}$$

3. Analytical Results of the Temperature Distribution

A complete evaluation of the numerous solutions to this problem was reference the method presented by Klinkenberg [24] and provides the source for the following relationships used to generate the results, which are

$\eta<2.0 \quad \xi<2.0$

$$\theta_f=1.0-\exp(-\eta-\xi)\sum_{n=1}^{n=\infty}\left(\frac{\xi^{nk=n-1}}{n!}\sum_{k=0}\frac{\eta^k}{k!}\right) \tag{12}$$

$2.0\le\eta<4.0 \quad 2.0\le\xi<4.0$

$$\theta_f=1.0-\frac{[1.0+\mathrm{erf}(\sqrt{\xi}-\sqrt{\eta})]}{2}-\frac{\xi^{0.25}\exp(-\eta-\xi)I_0(2\sqrt{\eta\xi})}{\xi^{0.25}+\eta^{0.25}} \tag{13}$$

$\eta\ge4.0 \quad \xi\ge4.0$

$$\theta_f=1.0-\frac{1}{2}[1.0+\mathrm{erf}(\sqrt{\xi}-\sqrt{\eta}-\xi^{-0.5}/8-\eta^{-0.5}/8)] \tag{14}$$

As pointed out by Larsen [23], the equations used in the description of the simplified mathematical model of the heat storage unit are symmetric. Therefore, the value of the non-dimensional temperature in the solid material can be obtained by using

$$\theta_m(\eta,\xi)=1.0-\theta_f(\xi,\eta) \tag{15}$$

The non-dimensional temperature distributions for the segmental plate in the rotary air preheater are shown in Fig. 2 based on Eqs. (13) to (15), as a function of non-dimensional length, ξ, and non-dimensional time, η. The following observations may be made from this figure: (1) in each case, the non-dimensional temperature for the segmental plate is uninterrupted, which increased gradually with the non-dimensional length, ξ, increasing and is decreased while increasing the non-dimensional time, η. The maximum value appears near the cold end of the air preheater in which there is an obvious decrease resulting from its resistance. (2) the nonlinearities first appeared at small values of η and grew as ξ increased. As η the increases, the deviation from a linear response becomes significant in the range of $2<\eta<4$, and deterioration of the linear tendency appeared throughout the complete range of variables.

A comparison of the values of the non-dimensional heat storage

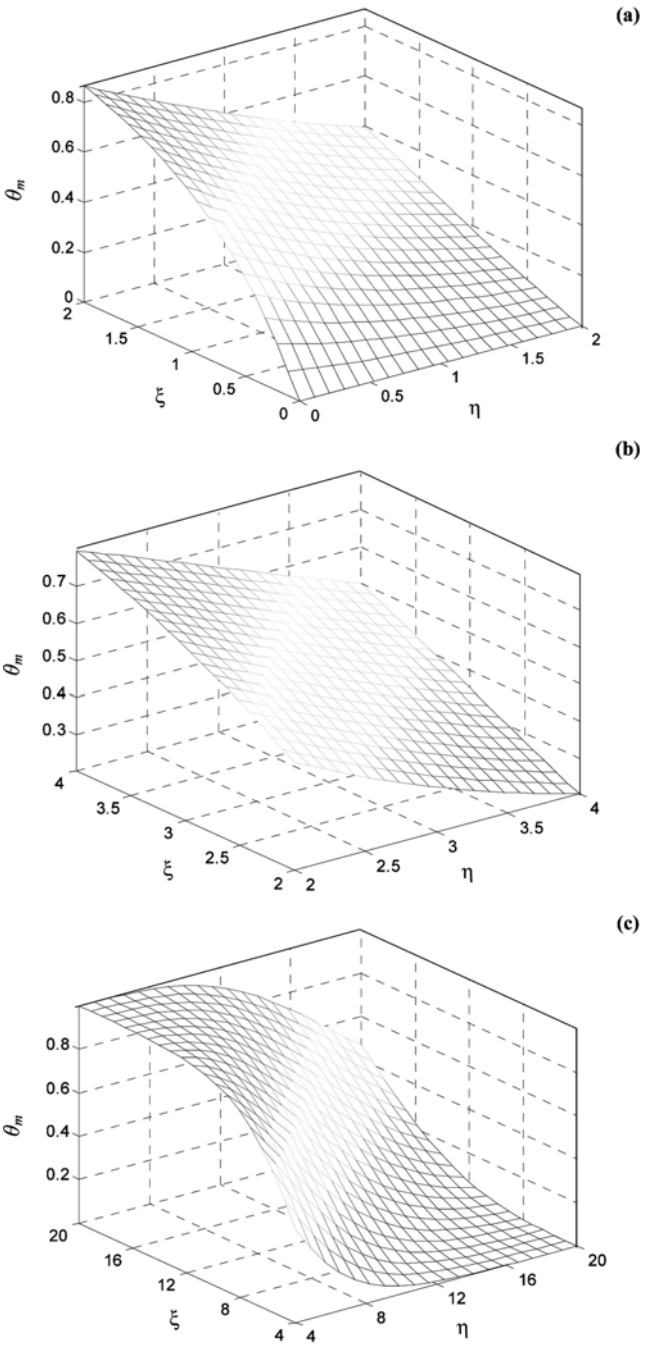

Fig. 2. Non-dimensional fluid and solid temperature distribution as a function of non-dimensional length (ξ) and non-dimensional time (η). (a) $0\le\eta<2.0$, $0\le\eta<2.0$, (b) $2.0\le\eta<4.0$, $2.0\le\xi<4.0$, (c) $\eta\ge4.0$, $\xi\ge4.0$.

obtained from the simplified method and the modified heat transfer coefficient method recommended by Schmidt and Szego [25,26] is presented in Table 1. In the case of ξ=4.8, the results obtained using the simplified model were in good agreement with the results obtained using the modified film coefficient method. Where as at ξ= 0.1, the most severe case, the agreement is not so close, although it is still considered to be within the acceptable limits. When evaluating the accuracy of the results obtained using the simplified method, it should be remembered that the simplified model was analyzed

Table 1. Comparison results of the fluid temperature distribution in calculational methods

ξ	Simplified		Modified heat transfer coefficient	
	η=0.1	η=4.8	η=0.1	η=4.8
0.5	0.4092	0.0812	0.4184	0.0800
1.0	0.6510	0.1173	0.6595	0.1147
2.0	0.8701	0.1837	0.8794	0.1835
2.5	0.9124	0.2409	0.9218	0.2400
3.0	0.9432	0.3204	0.9526	0.3201
5.0	0.9631	0.4561	0.9727	0.4537
7.5	0.9921	0.7394	0.9988	0.7391
10.0	0.9987	0.9173	1.0000	0.9712

in an attempt to identify the condition for which the material temperature has a linear timewise variation.

It can be seen that the simplified model can predict temperature surface on the segmental plates as well as inside of the materials. Furthermore, it should be noted that the method can be easily to be performed for various parametric conditions.

THERMAL STRESS DEFORMATION OF AIR PREHEATER

1. The Theory about Thermal Stress Model of Segmental Plate

It should be emphasized that all idealizations for the thermal stress in segmental plate, not only considering the horizontal thermal stress, the vertical thermal stress and the sheer stress in y direction should be also considered for entire stress analysis. Therefore, it is better to employ the classical thermo-elastic theory to analyze the entire segmental plate deformation, which includes the following three types of equations and boundary conditions [27].

(i) Coordination equation

$$\frac{\partial^4 F}{\partial x^4}+\frac{\partial^4 F}{\partial x^2\partial y^2}+\frac{\partial^4 F}{\partial y^4}=-\alpha E\left(\frac{\partial^2 t}{\partial x^2}+\frac{\partial^2 t}{\partial y^2}\right) \tag{16}$$

$$F|_\Gamma=\partial F/\partial n|_\Gamma=0 \tag{17}$$

$$\sigma_x=\frac{\partial^2 F}{\partial y^2};\quad \sigma_y=\frac{\partial^2 F}{\partial x^2};\quad \tau_{xy}=-\frac{\partial^2 F}{\partial x\partial y} \tag{18}$$

(ii) Structural equation

$$\varepsilon_x=(\sigma_x-v\sigma_y)/E+\alpha t \tag{19}$$

$$\varepsilon_y=(\sigma_y-v\sigma_x)/E+\alpha t \tag{20}$$

$$\gamma_{xy}=2(1+\nu)\tau_{xy}/E \tag{21}$$

(iii) Geometric equations

$$\varepsilon_x=\partial U/\partial x \tag{22}$$

$$\varepsilon_y=\partial V/\partial y \tag{23}$$

$$\gamma_{xy}=\partial U/\partial y+\partial V/\partial x \tag{24}$$

(iv) Boundary conditions

If x=0, then U=0 (25)

If x=0, y=0, then V=0 (26)

where $\partial F/\partial n|_\Gamma$ is thermal stress function.

With Eqs. (9) and (15), it is easier to derive the temperature of segmental plate t_m (or t) as a function of coordinate *y*, and can be expressed by Maclaurin series, where a_1, a_2, … are constants and n is assumed to be even number by Drobnic [28].

$$t=\sum_{k=0}^{n} a_k y^k \tag{27}$$

Eqs. (16) to (25) form the analytical model, which used to simulate the thermal stress deformation of a rotary air-preheater.

2. Analytical Solution on the Thermal Stress Model of Segmental Plate

The implicit analytical method is utilized to solve the equations of classical thermo-elastic model developed above. Substituting t of Eq. (27) into Eq. (16) reduces to

$$F=-\alpha E\left\{\sum_{k=0}^{n}\left[\frac{a_k y^{k+2}}{(k+1)(k+2)}\right]+\frac{1}{6}b_1y^3+\frac{1}{2}b_2y^2+b_3y+b_4\right\} \tag{28}$$

$$\sigma_x=-\alpha E\left[\sum_{k=0}^{n} a_k y^k+b_1y+b_2\right] \tag{29}$$

where σ_y and τ_{xy} are zero. By solving geometric equation, b_1, b_2, U and V can be expressed as Eqs. (30)- (33)

$$b_1=\frac{3}{c^3}\sum_{k=1}^{n/2}\left[\frac{a_{2k-1}c^{2k+1}}{2k(2k+1)}\right]-\frac{3}{2c^3}\sum_{k=1}^{n/2}\left[\frac{a_{2k-1}}{2k}c^{2k}\right] \tag{30}$$

$$b_2=-\frac{1}{c}\sum_{k=1}^{n/2}\left[\frac{a_{2k}}{2k(2k+1)}c^{2k+1}\right] \tag{31}$$

$$U=-\alpha(b_1y+b_2)x+f_1(y) \tag{32}$$

$$V=\alpha(1+\nu)\sum_{k=0}^{n}\left(\frac{a_k y^{k+1}}{k+1}\right)+\alpha\nu\left(\frac{b_1}{2}y^2+b_2y\right)+f_2(y) \tag{33}$$

To get complete solution, $f_1(y)$ and $f_2(y)$ should be determined. Using Eqs. (17) and (22), the two unknown functions $f_1(y)$ and $f_2(y)$ can be shown as in Eq. (34)

$$\frac{df_1}{dy}-\alpha b_1x+\frac{df_2}{dx}=0 \tag{34}$$

Eq. (34) is tenable for every values of x and y in their ranges respectively, so there must be existed relationship of Eq. (35), where d_0 is undetermined constant.

$$\frac{df_1}{dy}=\alpha b_1x-\frac{df_2}{dx}=d_0 \tag{35}$$

Then the solution of $f_1(y)$ and $f_2(y)$ are expressed as in Eqs. (36) and (37), where d_1 and d_2 are also undetermined constants.

$$f_1=d_0y+d_1 \tag{36}$$

$$f_2=\alpha b_1x^2/2+d_0x+d_2 \tag{37}$$

Utilizing the boundary conditions of displacement, $d_0=d_1=d_2=0$ can be obtained. By substituting three constants into Eqs. (28) and (31), thermal strain can be written as in Eqs. (38) and (39)

$$U=-\alpha(b_1y+b_2)x \tag{38}$$

$$V=\alpha(1+\nu)\sum_{k=0}^{n}\left(\frac{a_k}{k+1}y^{k+1}\right)+\alpha\nu\left(\frac{b_1}{2}y^2+b_2y\right)+\frac{1}{2}\alpha b_1x^2 \quad (39)$$

For arbitrary point (x_0, y_0) on the segmental plate, the position of thermal deformation (x_1, y_1) can be expressed as in Eqs. (40) and (41)

$$x_1=x_0+U \quad (40)$$

$$y_1=y_0+V \quad (41)$$

The simplified relationship of Eqs. (40) and (41) are suitable for designing and analysis the clearance of thermal stress deformation for rotary air-preheater.

RESULTS AND DISCUSSION

To validate the model of thermal stress is effective, a rotary air-preheater operating in a thermal power plant is chosen. The geometrics, heat transfer coefficients, physical properties of the matrix material for air preheater as well as the fluid flow rates and inlet temperatures for the hot and cold fluid streams are provided in Table 2.

If the rotary air preheater is an equivalent hot gas maintaining the same actual heat transfer rate of the cold air. The temperature distribution for the segmental plate is continuous in the hot period and cold period respectively; the thermal stress should be sequential also in the whole rotating period [29]. Therefore, the focus is placed on the two transitional interfaces: one is the segmental plate rotates from the hot gas into the cold air; the other is that the segmental plate rotes out of the cold air and entering to the hot gas.

Firstly, the temperature distributions of the segmental plate in the two transitional interfaces are expressed by Maclaurin series and shown in Fig. 3. Then, the thermal stress deformation can be determined based on the temperature distribution of the segmental plate. Horizontal and vertical thermal stress deformations of segmental plate at two transitional interfaces are shown in Fig. 4.

Table 2. Physical properties of matrix material and working fluid

Parameter description	Value
Rotary air preheater	
Radius of the rotor (m)	4.160
Height of the rotor (m)	3.420
Packing density ($m^2 \cdot m^{-3}$)	402.3
Porosity	0.859
Fluids	
Gas inlet temperature (°C)	362
Gas flow rate ($kg \cdot s^{-1}$)	51.1
Gas-side heat transfer coefficient ($W \cdot m^2 \cdot °C^{-1}$)	82.2
Cold air inlet temperature (°C)	24
Air flow rate ($kg \cdot s^{-1}$)	42.4
Air-side heat transfer coefficient ($W \cdot m^2 \cdot °C^{-1}$)	72.7
Matrix	
Density ($kg \cdot m^3$)	7841
Temperature distribution at gas-side (°C)	
$t_h=-3.13y^4+8.85y^3-40.92y^2+126.94y+254.53$	
Temperature distribution at air-side (°C)	
$t_c=-3.13y^4+8.85y^3-40.94y^2+173.25y+181.58$	
Specific heat ($J \cdot kg \cdot °C^{-1}$)	456
Thermal conductivity ($W \cdot m \cdot °C^{-1}$)	50.3
linear expansion coefficient ($m \cdot °C^{-1}$)	13.23×10^{-6}
Young's modulus (Pa)	1.88×10^{11}
Poisson's ratio	0.26

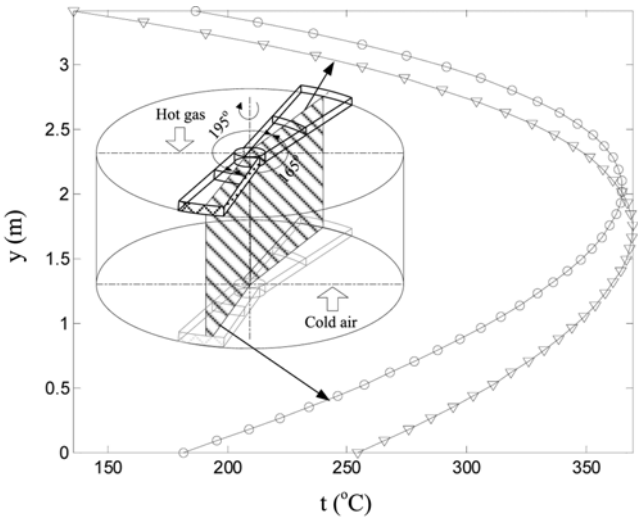

Fig. 3. The temperature distributions of segmental plate at two transitional interfaces.

The horizontal thermal deformation in y direction is shown in Fig. 4(a) and (c). It can be found that the horizontal deformation is ranged between –0.025 m (clockwise) and 0.025 m (counter clockwise) approximately. The maximum deformation lies in outer brim of hot end as rotor passing through from gas side to air side. Fig. 4(b) and (d) shows the vertical thermal deformation in x direction. The maximum value of vertical deformation is ranged from –0.021 m to 0.003 m which is in agreement basically with analytical results after comparison. The maximum deformation is still found to locate outer brim of hot end when air preheater rotates from hot gas side to cold air side. According to the deformation results of segmental plate in Fig. 4, even the temperature and operating conditions on both sides of rotor are different, and the magnitude of thermal expansion is not similar. It can be clearly seen that the horizontal and vertical deformations of segmental plate are in the same magnitude and the maximum value occurs in the same place. Furthermore, as to the rotor produces mushroom deformation, the main region of the radial seal leakage is located at hot end (hot gas inlet), since the thermal deformation of the rotor at this region has the largest value. Curve shape of hot end radial clearance looks like a triangle which hypotenuse expands gradually. The leakage area should be modified to minimize the leakage area when the thermal system is operating at different load. It should be emphasized that during rotary air pre-heater installation, the reserve value of radial clearance in the cold state should be adjusted momentarily according to the thermal stress deformation calculated in analytical method. The ideal position is that the segmental plate are in the immediate touch of the critical state to keep the leakage area is zero, it will considerably reduce the rotary air pre-heater leakage, and enhance improving the system efficiency.

In order to determine the reserve of seal clearance in the cold state,

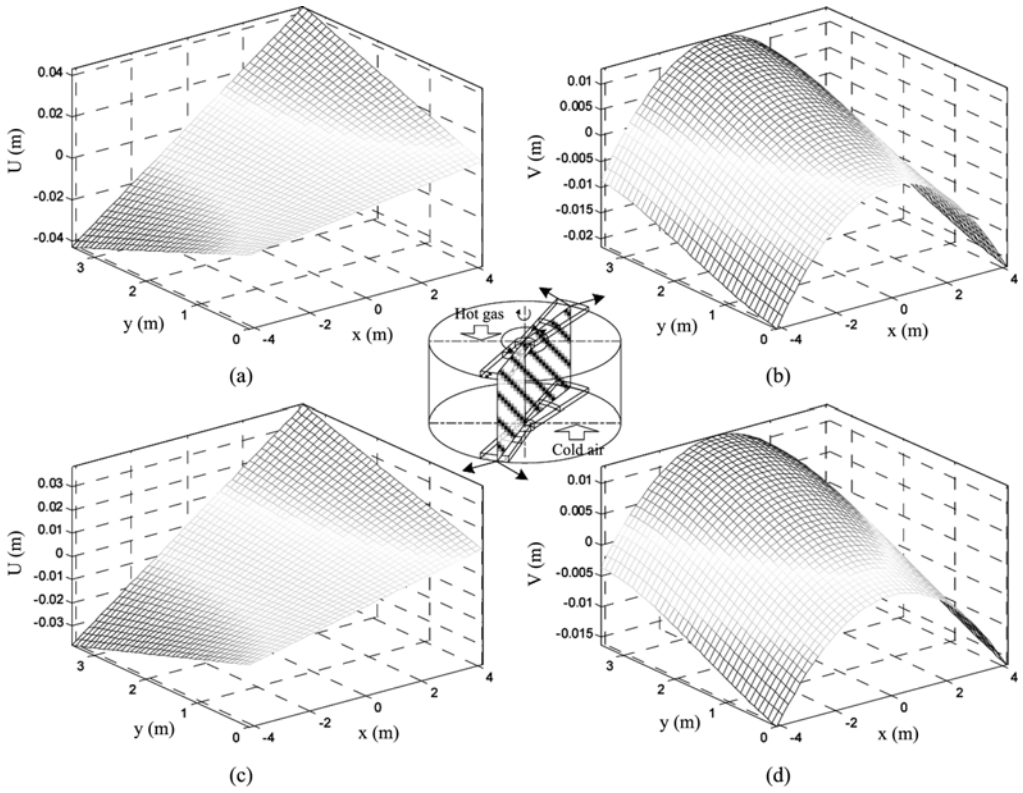

Fig. 4. Horizontal deformation U and Vertical deformation V as a function of radial coordinate (x) and height of rotor (y) for the segmental plates at two transitional interfaces.

comprehensive factors should be considered, not only the segmental plate thermal stress deformation, the rotor center tube elongation, but also the rotor shell deformation and the design surplus. According to the VN (Vertical Nonadjustable seal partition plate) design parameters of air-preheater [30], the elongations of the rotor center tube and of the shell are smaller than the thermal stress deformation of the segmental plate. Therefore, a suitable surplus value can be considered to be added on the design parameter. The calculation results of the radial seal clearance with the formula above mentioned, and the values of VN designing company introduced are compared in Fig. 5. As can be seen from Fig. 5, Most relative discrepancy of the data is in the range of 1-5%. If considering the value of the design surplus, the calculation results of thermal deformation of the model rotor are in good agreement with the value presented by VN designing company. It indicates that the analytical method of the thermal stress deformation for rotary air-preheater has its scientific precision and can be used to the actual engineering system. It not only provides theoretical reference for the adjustment of the gap to be sealed and the reserve of the clearance to improve the system efficiency, but also can be served for simplifying the control system of air-preheater in the thermal power plant.

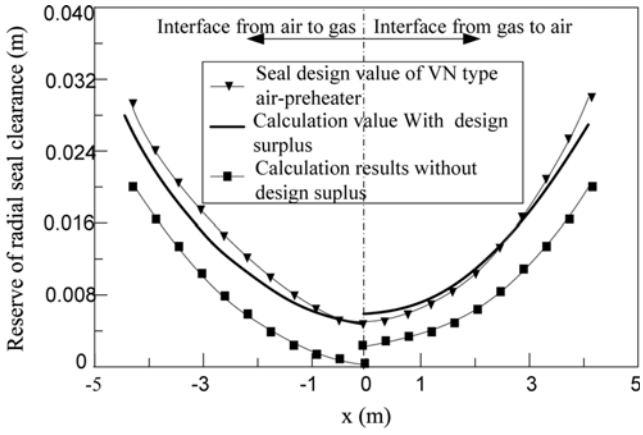

Fig. 5. The comparison of reserved value and calculation results of radial seal clearance for segmental plate.

CONCLUSIONS

In order to install the rotary air-preheater correctly with the precise reserve of the seal clearance and to equip with effective seal control system, the mushroom deformation of the air-preheater rotor has been analyzed with thermal stress deformation theory.

(1) A simplified mathematical model on the temperature distribution was established; the results show that the non-dimensional temperature for the segmental plate is increased with the non-dimensional length, ξ, increasing and decreased while increasing the non-dimensional time, η.

(2) Nonlinearities first appeared at small values of η and grew as ξ increased. As η increasing, the deviation from a linear response becomes significant and deteriorates throughout the complete range.

(3) The temperature distribution is employed to investigate the thermal stress deformation of the segment plate in rotary air pre-

heater. With the help of the thermal elasticity theory, the formulas determining the thermal deformation of segmental plates are concluded. The results show that the maximum deformation is 25 mm for horizontal and 21 mm for vertical direction and locate outer brim of hot end when air preheater rotates from hot gas side to cold air side.

(4) Compared with the actual rotary air preheater operation commercial thermal power plant, it can be concluded that the mathematical model on the segmental plate thermal deformation is reasonable. The analytical results can provide detailed and reliable data for sealing control system. Furthermore, the leakage problem can be effectively reduced.

ACKNOWLEDGMENTS

The research is the outcome of the fostering project of the Best Lab in the area of IGCC supported financially by the ministry of commerce, Industry and Energy (MOCIE).

NOMENCLATURE

A : heat transfer area [m^2]
c : specific heat ($J \cdot kg \cdot {}^oC^{-1}$]
c : half height of matrix [m]
E : young's modulus [Pa]
f : auxiliary function
F : deformation function
h : heat transfer efficient [$W \cdot m^2 \cdot {}^oC^{-1}$]
I : mass moment of inertia [$kg \cdot m^2$]
L : matrix (rotor)'s height [m]
M : torque of segmental plate [N·m]
P : tensile pressure [Pa]
R : radius of rotor [m]
S : cross-sectional area [m^2]
t : temperature [°C]
U : horizontal deformation of matrix [m]
V : vertical deformation of matrix [m]
x : radial direction of rotor
y : height direction of rotor

Greek Letters

α : linear expansion coefficient [$m \cdot {}^oC^{-1}$]
δ : thickness of matrix [m]
γ : angular distortion
ε : thermal strain
η : non-dimensional time
θ : non-dimensional temperature
ξ : non-dimensional length
ρ : density [$kg \cdot m^3$]
s : thermal stress [MPa]
Γ : boundary of segment plate
τ : shear stress [MPa]
τ : times [s]
ν : poisson ratio

Subscript

c : cold air
f : fluid
h : hot gas
i : inlet, entering
m : metal or matrix
o : outlet, leaving

REFERENCES

1. R. S. Shah, *Applied Thermal Engineering*, **19**, 685 (1999).
2. Z. Y. Chang, *Mechanism and Machine Theory*, **36**, 143 (2001).
3. T. Kant, *Journal of Thermal Stresses*, **17**, 229 (1994).
4. T. Skeipko, *Heat Transfer Eng.*, **18**, 56 (1997).
5. T. Skiepko, *Heat Recov. Syst*., **8**, 469 (1998).
6. T. Skiepko, *Heat Transfer Eng*., **27**, 14 (1993).
7. V. I. Gromovyk, *J. Appl. Maths Mechs*., **59**, 159 (1995).
8. M. Sunar, *J. of Mat. Pro. Tech.*, **123**, 172 (2006).
9. A. Robaldo, *Computers and Structures*, **84**, 1236 (2006).
10. F. A. Creswick, *Ind. Math.*, **8**, 61 (1957).
11. J. R. Mondt, *ASME J. Eng. Power*, **86**, 121 (1964).
12. T. J. Lambertson, *Trans. ASME*, **15**, 57 (1957).
13. W. M. Kays, McGraw Hill Co. (1984).
14. G. D. Banke, *ASME, J., Eng., Power*, **86**, 105 (1964).
15. N. Ghodsi, *Applied Thermal Engineering*, **23**, 571 (2003).
16. M. Djuric and J. Hung. *Indus. Chem.*, **17**, 1 (1989).
17. K. C. Leong, *Heat Recov. Syst. CHP*, **11**, 461 (1991).
18. D. S. Beck, *Trans. ASME*, **116**, 574 (1994).
19. G. D. Bahnke, *ASME J. Eng. Power*, **86**, 105 (1964).
20. A. J. Willmott, *Journal Institute of Energy*, **66**, 54 (1999).
21. T. Skiepko, *Int. J. Heat Mass Transf.*, **31**, 2227 (1988).
22. T. Skiepko, *Int. J Heat Mass Transf.*, **32**, 1443 (1989).
23. F. W. Larson, *Int. J. Heat Mass Transf.*, **10**, 149 (1967).
24. A. Klinkenberg, *Ind. Eng. Chem.*, **46**, 2286 (1954).
25. F. W. Schmidt, *Int. J. Heat Mass Transf.*, **100**, 737 (1978).
26. J. Szego, *Int. J. Heat Mass Transf.*, **100**, 740 (1978).
27. D. Y. Yoon, K. H. Choi, Y. H. Kim and L. H. Kim, *Korean J. Chem. Eng.*, **25**, 217 (2008).
28. B. J. Drobnic, *Int. J. Heat Mass Transf.*, **10**, 161 (2006).
29. S. Poncet, *Int. J. Heat Mass Transf.*, **50**, 1528 (2007).
30. http://www.howden.com/en